Analysis of Transition Mechanism of Cubic Boron Nitride Single Crystals under High Pressure-High Temperature with Valence Electron Structure Calculation *

Mei-Zhe Lv(吕美哲)[1], Bin Xu(许斌)[2**], Li-Chao Cai(蔡立超)[1], Feng Jia(贾凤)[2], Xing-Dong Yuan(袁兴栋)[2]

[1]*School of Materials Science and Engineering, Shandong University, Jinan 250101*
[1]*School of Materials Science and Engineering, Shandong Jianzhu University, Jinan 250101*

(Received 13 September 2018)

The possibilities of hexagonal boron nitride (hBN) and lithium boron nitride (Li_3BN_2) transition into cubic boron nitride (cBN) under synthetic pressure 5.0 GPa and synthetic temperature 1700 K are analyzed with the use of the empirical electron theory of solids and molecules. The relative differences in electron density are calculated for dozens of bi-phase interfaces hBN/cBN, Li_3BN_2/cBN. These relative differences of hBN/cBN are in good agreement with the first order of approximation (<10%), while those of Li_3BN_2/cBN are much greater than 10%. This analysis suggests that Li_3BN_2 is impossible to be intermediate phase but is a catalyst and cBN should be directly transformed by hBN.

PACS: 31.15.bu, 64.70.mf, 61.50.Ah, 31.15.bt DOI: 10.1088/0256-307X/36/1/013101

At present, the static high pressure-high temperature (HPHT) catalytic method is most commonly used to synthesize cubic boron nitride (cBN) with hexagonal boron nitride (hBN) as starting materials and with lithium nitride as catalysts on an industrial scale.[1–3] The transition mechanism has been discussed in some studies and some models are proposed by considering the possibility of phase transition between similar structures or by presuming the transition process with some indirect experimental results.[4,5] The two main transition mechanisms are that cBN can be directly transformed from hBN and cBN can be precipitated from solvent.[6,7] Namely, in the Li_3N-hBN system, cBN can be transformed by hBN or be dissolved by Li_3BN_2. Thus, it is very desirable to study the relationships of hBN→cBN, Li_3BN_2→cBN+Li_3N to understand the phase transition mechanism of cBN.

The empirical electron theory (EET) of molecules and solids[8] is established by Yu, based on Pauling's valence bond theory. The EET has successfully been applied to many aspects of materials research (e.g., phase diagrams, phase transition, hot working, physical properties).[9–11] However, the phase transition of cBN is rarely reported with the use of EET. The electron structures and electron densities of solid and molecules can be calculated by means of the bond length difference method (BLD) presented in EET. Meanwhile, the improved Thomas–Fermi–Dirac theory by Cheng (TFDC)[12] proposes that the boundary condition between atoms is simply the continuity of the electronic densities. Electron density is considered to be a bridge connecting EET and TFDC,[13] thus the two theories could be used to discuss the cBN transition mechanism by analyzing the continuity of electron density between bi-phase interfaces hBN/cBN and Li_3BN_2/cBN under the conditions of cBN synthesis.

The experimental bond length $D_{n\alpha}$ in lattice structures can be confirmed, knowing the atom sites and the lattice parameters. The fractional coordinates of atoms u and v in crystal structures can be expressed in $(x_u y_u z_u)$ and $(x_v y_v z_v)$, respectively. Due to the EET, the bonds ($D_{n\alpha} > 0.5$ nm) rarely have an effect on the results, and thus can be ignored. The value of $D_{n\alpha}$ can be obtained by

$$D_{n\alpha}^{u-v} = [(x_u - x_v)^2 a^2 + (y_u - y_v)^2 b^2 + (z_u - z_v)^2 c^2]^{1/2}. \quad (1)$$

According to the main equations for the BLD method in EET, Eq. (1) can be expressed as

$$D_{nA}^{u-v} = R_u(1) + R_v(1) - \beta \log n_A, \quad (2)$$

$$D_{n\alpha}^{s-t} = R_s(1) + R_t(1) - \beta \log n_\alpha \quad (\alpha = B \ldots N), \quad (3)$$

$$\log \frac{n_\alpha}{n_A} = \{(D_{nA}^{u-v} - D_{n\alpha}^{s-t}) + (R_s(1) + R_t(1)) - (R_u(1) + R_v(1))\}/\beta, \quad (4)$$

where n_α is the covalent electron pairs of the α bond, $R(1)$ is the bond radius which can be gained from the hybridization table in EET, and β is a coefficient. The ratio of covalent electron distribution on bonds $\gamma_\alpha = \frac{n_\alpha}{n_A}$ can be calculated by Eq. (4), which can be obtained by subtracting Eq. (2) from Eq. (3). The values of n_A and n_α can be calculated by

$$\Sigma n_c = \Sigma I_\alpha n_\alpha = n_A \Sigma I_\alpha \gamma_\alpha, \quad (5)$$

where n_c is the total valence electron number of a crystal plane, which is equal to the total number of electrons distributed on all covalent bonds, I_α represents equivalent bond number of bond α on the plane, which means that the covalent bonds have the equivalent bond length and uniform environment.

According to EET, the covalent electron density of a certain crystal plane can be calculated by

$$\rho = \frac{\Sigma n_c}{S} = \frac{\Sigma I_\alpha n_\alpha}{S}, \quad (6)$$

where S is the area of the crystal plane. The relative differences in electron density of an interface can be

*Supported by the National Natural Science Foundation of China under Grant No 51272139.
**Corresponding author. Email: xubin@sdjzu.edu.cn
© 2019 Chinese Physical Society and IOP Publishing Ltd

defined as follows:

$$\Delta\rho = \frac{|\rho_1 - \rho_2|}{(\rho_1 + \rho_2)/2} \times 100\%. \quad (7)$$

The bond energy E_a of covalent bond formed by two atoms (u and v) in crystals is calculated by

$$E_a = \sqrt{b_u b_v} \cdot \sqrt{f_u f_v} \frac{n_\alpha}{\overline{D}_\alpha}, \quad (8)$$

where b is a coefficient, which represents the shielding factor of the electron to nuclear charge, whose value can be found in Ref. [8]. The value of f represents the bond-forming ability of the atom hybrid orbital, which can be gained by

$$f = \sqrt{\alpha} + \sqrt{3\beta} + \sqrt{5\gamma},$$
$$\alpha = \frac{n_s}{n_T},\ \beta = \frac{n_p}{n_T},\ \gamma = \frac{n_d}{n_T}, \quad (9)$$

where n_s, n_p, n_d represent the valence electrons of s, p and d, respectively, and n_T represents the total valence electron number, whose values are gained in Ref. [14].

The BLD method is excessively dependent on the accurate lattice parameters (a, b, c), which are influenced by the promotion of synthetic pressure and synthetic temperature. Different p-T areas of cBN growth in the Li_3N-hBN system have been proposed, which may be related to the purity and degree of order of hBN and the synthesis process. Considering the real synthesis condition and previous experimental results, 5.0 GPa and 1700 K are selected as the calculated pressure and calculated pressure, because stable cBN can exist in this region. In our previous work,[15] the calculations of lattice parameters have been performed using the Vienna ab-initio simulation package (VASP). The projector-augmented wave with generalized gradient approximation (PAW-PBE) was employed separately to calculate hBN, cBN and Li_3BN_2 at HPHT (5.0 GPa and 1700 K). A plane wave kinetic energy cut-off value of 700 eV was correspondingly used to ensure a total-energy convergence of 10^{-5} eV/atom, and $9 \times 9 \times 3$, $9 \times 9 \times 9$, $9 \times 9 \times 8$ Monkhorst-pack k-points meshes were, respectively, employed to hBN, cBN and Li_3BN_2. The calculated results are in good agreement with the previous experimental studies, and this accrues the reliability of the calculation methods employed in this work for the lattice parameters of three structures. The lattice parameters of hBN are $a = 0.24940$ nm, $c = 0.60627$ nm, the lattice parameter of cBN is 0.36352 nm, and the lattice parameters of Li_3BN_2 are $a = 0.44378$ nm, $c = 0.50265$ nm at 5.0 GPa and 1700 K.

The BLD method is efficient to determine the state group of every possible existent atom which must satisfy the difference between $D_{n\alpha}$ and theoretical bonding length $\overline{D}_{n\alpha}$ is lower than 0.005 nm ($\Delta D_{n\alpha} = |\overline{D}_{n\alpha} - D_{n\alpha}| < 0.005$ nm) and this means that the condition for stable valence electron structure of a crystal is $\Delta D_{n\alpha} < 0.005$ nm. Using the BLD method, their (hBN, cBN and Li_3BN_2) average valence electron structures of all qualified hybrid order could be obtained. The average valence electron structures of all qualified hybrid order are more accurate to analyze the properties and behavior of crystals.[9–11] The transition to cBN starts with displacement of atoms of the hBN or Li_3BN_2 phases which depends on their stability. The larger the structure stability, the greater the difficulty to break up the covalent bonds of structure units. The formation and breakup of covalent bonds of structure units can be characterized by the covalent electron pairs (n_A) and the bond energy (E_A) of the strongest covalent bond. For hBN and Li_3BN_2, the strongest covalent bonds are both B–N bonds. Their corresponding values of n_A (hBN and Li_3BN_2) are 1.20756, 2.32482. According to Eq. (8), E_A for hBN and Li_3BN_2 are calculated to be 166.28 kJ/mol and 345.05 kJ/mol, respectively. The results show that the values of n_A and E_A of Li_3BN_2 are much greater than those of hBN, which means that Li_3BN_2 is more stable than hBN under the condition of cBN transition. Because n_A and E_A are larger,[10,11] a greater driving force is needed to break up the bond of D_{nA}, thus the transition of $Li_3BN_2 \rightarrow$ cBN is more difficult than the reaction of hBN$\rightarrow$cBN.

Table 1. Covalent electron density of crystal planes in hBN at 5.0 GPa and 1700 K.

Crystal planes	Bond	$D_{n\alpha}$ (nm)	n_α	I_α	$\sum n_c$	S (nm^2)	ρ (nm^{-2})
(0001)	A	0.14399	1.20756	6	7.80459	0.05387	144.88611
	B	0.24940	0.05096	6			
	C	0.25147	0.03092	6			
	D	0.28798	0.01132	6			
$(10\bar{1}0)$	B	0.24940	0.05096	2	0.19451	0.15121	1.28636
	C	0.24940	0.03092	2			
	E	0.30314	0.00692	4			
	H	0.39254	0.00038	8			
$(11\bar{2}0)$	A	0.14399	1.20756	4	4.95231	0.26190	18.90941
	D	0.28798	0.01132	4			
	E	0.28798	0.00692	8			
	F	0.30314	0.00311	4			
	G	0.33560	0.00189	4			
	I	0.41812	0.00021	4			
	J	0.41812	0.00013	4			
$(01\bar{1}2)$	B	0.24940	0.05096	2	0.16529	0.09842	1.67947
	C	0.25147	0.03092	2			
	H	0.39254	0.00038	4			

Table 2. Covalent electron density of crystal planes in cBN at 5.0 GPa and 1700 K.

Crystal planes	Bond	$D_{n\alpha}$ (nm)	n_α	I_α	$\sum n_c$	S (nm^2)	ρ (nm^{-2})
(100)-B	B	0.25705	0.04236	8	0.34959	0.13215	2.64547
	E	0.36352	0.00134	8			
(100)-N	C	0.25705	0.02654	8	0.21901	0.13215	1.65734
	F	0.36352	0.00084	8			
(111)-B	B	0.25705	0.04236	12	0.50943	0.11444	4.45144
	H	0.44522	0.00009	12			
(111)-N	C	0.25705	0.02654	12	0.31915	0.11444	2.78874
	I	0.44522	0.00006	12			
(110)	A	0.15741	0.84576	8	7.11424	0.18688	38.06774
	B	0.25705	0.04236	4			
	C	0.25705	0.02654	4			
	D	0.30141	0.00793	8			
	E	0.36352	0.00134	4			
	F	0.36352	0.00084	4			
	I	0.44522	0.00006	8			

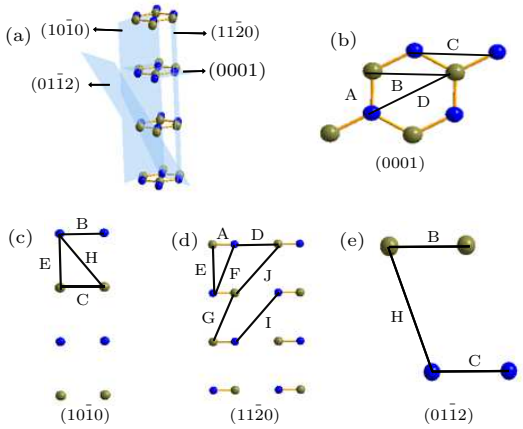

Fig. 1. (a) The main low-index planes of hBN crystals. (b)–(e) The distributions of atoms and covalent bonds in (0001), (10$\bar{1}$0), (11$\bar{2}$0) and (01$\bar{1}$2) planes of hBN, respectively.

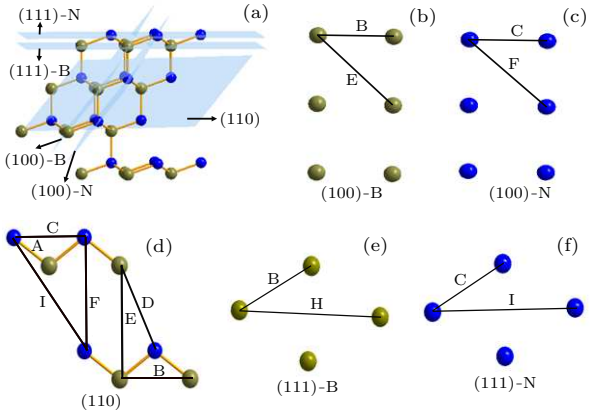

Fig. 2. (a) The main low-index planes of cBN crystals. (b)–(f) The distributions of atoms and covalent bonds in (100)-B, (100)-N, (110), (111)-B and (111)-N planes of cBN, respectively.

The lattice electron density can be obtained by Eq. (6), which is the ratio of the total lattice electron number and the total valence electron number in a cell. The three selected planes of Li_3BN_2 contain maximum the number of B atoms or N atoms. It is worth mentioning that as the (100) and (111) planes of cBN are polar, there are in total five structural models about cBN. Figures 1–3 show the distribution of atoms and covalent bonds in main low index planes of hBN, cBN and Li_3BN_2, respectively. Based on the calculation in Eqs. (6) and (7), the electron densities of different crystal planes in hBN, cBN and Li_3BN_2 crystals are listed in Tables 1–3, respectively, and Tables 4 and 5 show the relative differences in electron density of different bi-phase interfaces in hBN/cBN and Li_3BN_2/cBN, respectively. As listed in Table 4, the value about relative difference in electron density at hBN (01$\bar{1}$2)/cBN (100)-N is 1.33%, which is lower than 10%. According to the TFDC, the electron density of (100) plane in hBN is continuous with (100) plane in cBN at the first order of approximation (<10%). The lower $\Delta\rho$ of two adjacent planes, the closer the covalent electron structure of interface, and the lower the driving force for transforming one structure into another. This indicates that driving force required for the direct transformation from hBN to cBN is low enough, and the differences of valence electron structure at hBN/cBN interface could induce direct transformation from hBN into cBN.

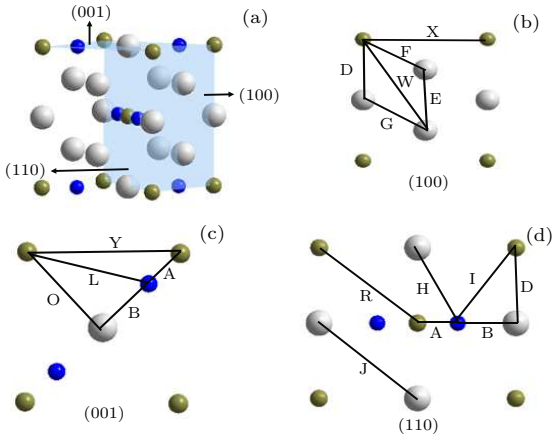

Fig. 3. (a) The main low-index planes of Li_3BN_2 crystals. (b)–(d) The distributions of atoms and covalent bonds in (100), (001) and (110) planes of Li_3BN_2, respectively.

As listed in Table 5, the minimum relative difference in electron density of all bi-phase interfaces at Li_3BN_2/cBN is 49.47%, which does not satisfy the first order of approximation (>10%). This indicates that Li_3BN_2 cannot be dissolved into cBN as the intermediate phase under the condition of 5.0 GPa and

1700 K. The value of $\Delta\rho$ of Li_3BN_2/cBN interfaces is larger, and thus the change of atom size on interface is greater. Therefore, a larger driving force of phase transition is needed under the HPHT synthetic process. These results are consistent with the previous thermal results[16] that the Gibbs free energy of hBN→cBN are negative, while those of Li_3BN_2→cBN are positive at the synthetic temperature and synthetic pressure of cBN single crystals. Because of its similar structure with cBN and larger lattice parameters, Li_3BN_2 can be the matrix of cBN nucleation, and thus decreases the surface energy between hBN and cBN.[17] The lattice of Li_3BN_2 is composed of Li1, Li2 and NBN^{-3} ions. The Li ions can attract outer electrons in N atoms from hBN and transfer them to B atoms under HPHT. The electron structures of B and N atoms have been changed from the sp^2 hybridized state into the sp^3 hybridized state.[16] The crystal defects trend to agglomerate at interfaces where $\Delta\rho$ is great,[14] hence, Li_3BN_2 can be adsorbed to the interior of cBN crystals, leading to the generation of internal defects in cBN crystals, which is beneficial for cBN gradual growth. Thus cBN single crystals are transformed from hBN directly with the catalysis of Li_3BN_2 at HPHT.

Table 3. Covalent electron density of common crystal planes in Li_3BN_2 at 5.0 GPa and 1700 K.

Crystal planes	Bond	$D_{n\alpha}$ (nm)	n_α	I_α	$\sum n_c$	S (nm^2)	ρ (nm^{-2})
(001)	A	0.13428	2.32482	4	13.40268	0.21701	61.76156
	B	0.19512	1.02226	4			
	L	0.35453	0.00198	4			
	O	0.38288	0.00073	8			
	Y	0.46582	0.00005	4			
	Z1	0.46582	0.00005	8			
(110)	A	0.13428	2.32482	4	14.49779	0.34761	41.70731
	B	0.19512	1.02226	4			
	D	0.26381	0.10256	8			
	H	0.29601	0.03877	4			
	I	0.32812	0.00433	8			
	J	0.32940	0.01222	8			
	R	0.42201	0.00019	8			
(100)	D	0.26381	0.10256	4	0.51130	0.24580	2.08020
	E	0.26381	0.00035	4			
	F	0.26769	0.00933	8			
	G	0.26769	0.00296	8			
	W	0.45920	0.00001	2			
	X	0.46582	0.00048	2			
	Y	0.46582	0.00005	8			

Table 4. Relative differences in electron density of hBN/cBN interfaces at 5.0 GPa and 1700 K. Here h represents hBN, and c represents cBN.

$\Delta\rho$ (%)	h(0001)	h(10$\bar{1}$0)	h(11$\bar{2}$0)	h(01$\bar{1}$2)
c(100)-B	192.83	69.13	150.91	44.67
c(100)-N	195.48	25.20	167.77	1.33
c(111)-B	188.08	110.32	123.78	90.43
c(111)-N	192.45	73.73	148.59	49.65
c(110)	116.73	186.93	67.30	183.11

Table 5. Relative differences in electron density of Li_3BN_2/cBN interfaces at 5.0 GPa and 1700 K. Here c represents cBN, and L represents Li_3BN_2.

$\Delta\rho$ (%)	L(001)	L(110)	L(100)
c(100)-N	90.27	190.61	189.69
c(100)-B	49.47	194.06	193.48
c(111)-B	126.62	184.44	182.95
c(111)-N	94.42	190.11	189.15
c(110)	189.77	97.12	89.67

By calculating $\Delta\rho$ of hBN/cBN and Li_3BN_2/cBN, it can be concluded that the reaction of hBN→cBN could be performed, while the reaction of Li_3BN_2→cBN is impossible under the condition of 5.0 GPa and 1700 K. The values of n_A and E_A of Li_3BN_2 are much larger than those of hBN, thus the greater driving force is needed for breaking up the bond of Li_3BN_2. These results show that cBN comes directly from the transformation of hBN but not from the decomposition of Li_3BN_2.

References

[1] Lv M Z et al 2018 *Appl. Surf. Sci.* **439** 780
[2] Wu W X et al 2008 *Acta Phys. Sin.* **57** 2486 (in Chinese)
[3] Yang D P et al 1993 *Diamond Relat. Mater.* **2** 174
[4] Hou L X et al 2012 *Appl. Surf. Sci.* **258** 3800
[5] Fukunaga O 2000 *Diamond Relat. Mater.* **9** 7
[6] Xu B et al 2015 *Integr. Ferroelectr.* **163** 139
[7] Wang Y L et al 2012 *Chin. Phys. B* **21** 060301
[8] Yu R H 1981 *Sci. Bull.* **26** 217 (in Chinese)
[9] Lin C et al 2016 *Comput. Mater. Sci.* **111** 41
[10] Lin C et al 2016 *Scr. Mater.* **117** 41
[11] Lin C et al 2015 *Comput. Mater. Sci.* **101** 168
[12] Cheng K J and Cheng S Y 1993 *J. Sci. Technol. Rev.* **12** 30 (in Chinese)
[13] Cheng K J and Cheng S Y 2001 *Theor. Appl. Fract. Mech.* **37** 19
[14] Zhang R L 1992 *The Empricial Electron Theory of Solid and Molecules* (Changchun: Jilin Science and Technology Press) p 478 (in Chinese)
[15] Xu B et al 2015 *Integr. Ferroelectr.* **162** 85
[16] Xu B et al 2014 *Entropy* **16** 912
[17] Yamane H et al 1987 *J. Solid State Chem.* **71** 1